Stanford Exploration Project, Report 115, May 22, 2004, pages 57–70

Ocean-bottom hydrophone and geophone coupling

Daniel A. Rosales and Antoine Guitton[1]

ABSTRACT

We compare two methods for combining hydrophone and geophone components for an ocean-bottom seismic experiment to eliminate the receiver ghosts associated with this type of seismic acquisition. One approach is in the time domain, the other in the frequency domain. Both approaches are compared with the 2D OBS data over the Mahogany field in the Gulf of Mexico. The receiver ghosts are eliminated more efficiently with the frequency domain method, because this method combines the data in two different steps: i) calibration, and ii) deghosting.

INTRODUCTION

Ocean-bottom cable acquisition results in a receiver ghost problem. An operational method to solve this problem is to use paired hydrophone and geophone detectors. Combining the hydrophone and geophone takes the advantage of the fact that the two types of detectors generate signals of the same polarity for the upcoming wavefield, and opposite polarity for the downgoing wavefield (Gal'perin, 1974; Barr and Sanders, 1989; Soubaras, 1996). The main challenge of this method is that the hydrophone and geophone must be properly calibrated to produce a deghosted output.

Barr and Sanders (1989) propose a technique in the time domain that calibrates the geophone measurement and eliminates the ghost reflection in one simple step. According to Soubaras (1996), however, the geophone calibration and the deghosting process must be done separately. He proposes a method in the frequency domain to separately calibrate the geophone measurement and eliminate the receiver ghost.

A 2D line over the Mahogany field in the Gulf of Mexico helps to test both of these approaches. First, we present a pre-processing technique over this 2D line. We present two methods of combining the hydrophone and geophone components and use the results to obtain preliminary estimates of the P velocity field for this dataset.

[1]**email:** daniel@sep.stanford.edu, antoine@sep.stanford.edu

PRE-PROCESSING

This section illustrates some of the problems with the Mahogany data set. Figure 1 shows the hydrophone (left) and the geophone (right) components of a common shot gather. Note the events with a predominantly linear moveout on the hydrophone component. These events represent an interface wave, one that travels in the first layer below the water bottom with a characteristic velocity of 1500m/s. Due to the high energy of these events and theirs dispersive characteristic it is not possible to observe and analyze the contribution of the far offset traces to the moveout of the reflections. Hence, it is important that we eliminate these events without destroying the main reflections. Because this noise has a characteristic linear moveout, a radial noise model serves to approximate and eliminate these events.

The pseudo-unitary implementation of the radial-trace transform (Brown and Claerbout, 2000) promises to be an efficient technique to suppress the noise in the hydrophone component, because the radial-trace transform lowers the apparent temporal frequency of these radial events.

After the radial noise suppression, we also performed a mute with the water velocity and a bandpass filter. Figure 2 shows the same gathers as in Figure 1 after the radial-trace noise suppression for the hydrophone component and the mute and bandpass filtering for both the hydrophone and geophone components. Now, it is possible to observe more clear reflections in the hydrophone component of the shot gather. Most of these events match with those observed in the geophone component of the shot gather.

HYDROPHONE AND GEOPHONE COMBINATION

We discuss two methods to combine the pressure and velocity detectors at an identical location on a 2D OBC line. Both methods perform a calibration over the velocity detector or geophone. The goal of both of these methods is to eliminate the ghost reflection. The first method is in the time domain and combines the geophone calibration and the deghosting in one step. The second method is in the frequency domain and performs the geophone calibration and the deghosting in two steps.

Time domain methodology

The method that Barr and Sanders (1989) proposed to combine the hydrophone and geophone is simple and easy to implement. They simply add the hydrophone and the calibrated geophone in the shot domain. The calibrated geophone is computed with a constant factor equal to the ratio of the amplitudes of the hydrophone and geophone. We calculate a constant factor per trace, we average all of them, and finally apply the averaged constant factor to the entire shot gather.

This procedure not only calibrates the geophone but also eliminates the ghost reflection.

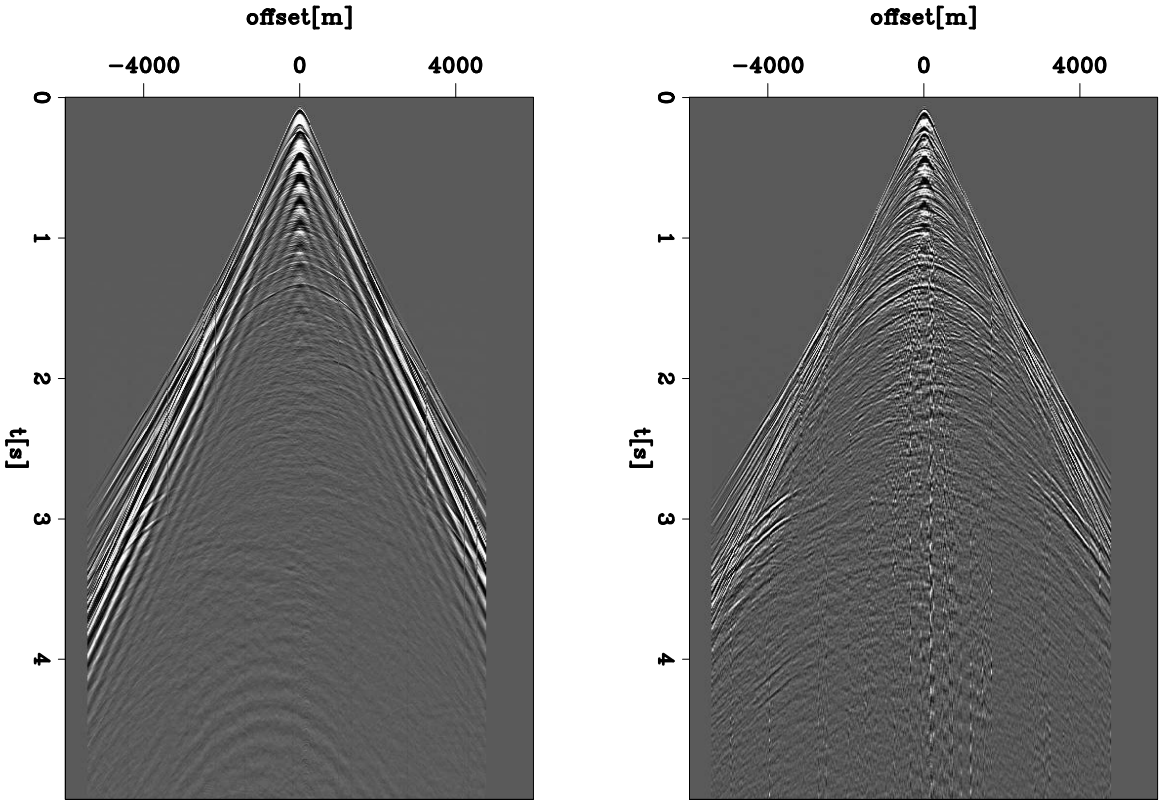

Figure 1: One common-shot gather for the Mahogany data set. The left panel shows the hydrophone component and the right panel shows the geophone component. daniel1-shots [CR]

The final combined signal ($s(t)$) is given by the following:

$$s(t) = h(t) + \frac{\rho v_p}{\cos\gamma_p'} \frac{kt(1+kr)}{kt(1-kr)} z(t), \tag{1}$$

where $h(t)$ and $z(t)$ correspond to the hydrophone and geophone, respectively, ρ is the water density, v_p is the P-wave water velocity, γ_p' is the P-wave refraction angle in water, and kr, kt are the reflection coefficient and the refraction coefficient, respectively.

Figure 3 presents the physical model for this approach. Solving the boundary conditions for the elastic wave-equation at the water bottom (left panel on Figure 3) gives the amplitudes of the reverberations (right panel on Figure 3). This model explains that combining the hydrophone and the geophone components as in equation (1) results in a reverberation-free signal.

The right panel on Figure 3 also explains how to obtain the scale factor for equation (1). Comparing the amplitudes of the reverberations shows that the scale factor is just the absolute value of the ratio between the amplitudes of the hydrophone and the geophone. The final result, $s(t)$, is a deghosted output.

Figure 4 shows the result of this approach over the common-shot gather from Figure 1.

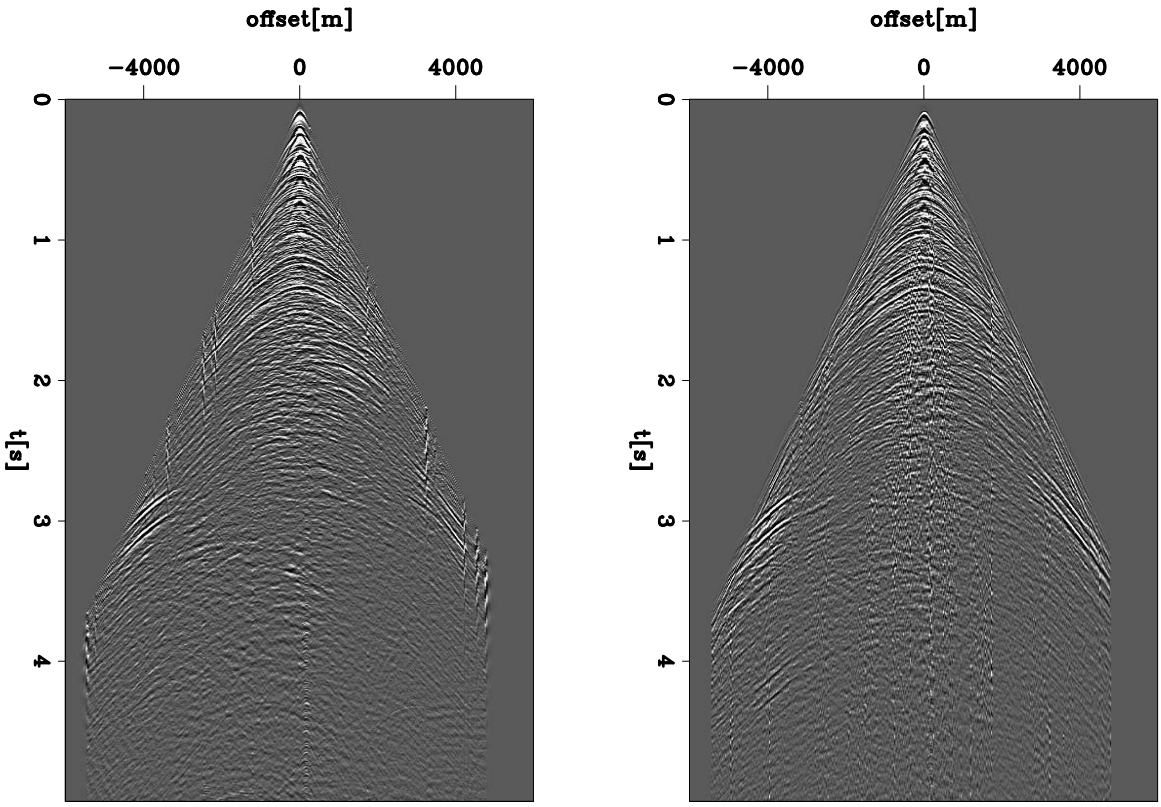

Figure 2: Same common-shot gather as in Figure 1, after simple pre-processing. daniel1-spro [CR,M]

Although it was possible to eliminate some of the multiples, the final result, $s(t)$, is not totally multiple-free.

Frequency domain methodology

Soubaras (1996) proposes to split into two procedures the calibration of the hydrophone and geophone and the ghost elimination. Figure 5 shows the physical model proposed by Soubaras (1996). The fields U_0, D_0, and S_0 represent the initial upgoing, downgoing and source wavefields, respectively. Similarly, the fields U, D, and S are the upgoing, downgoing and source wavefields at the water-bottom level (receiver level).

Calibration

The pressure component (P) and the vertical component (Z) of the receiver gather are both in the frequency domain. The available data are the hydrophone component (P) and the non-

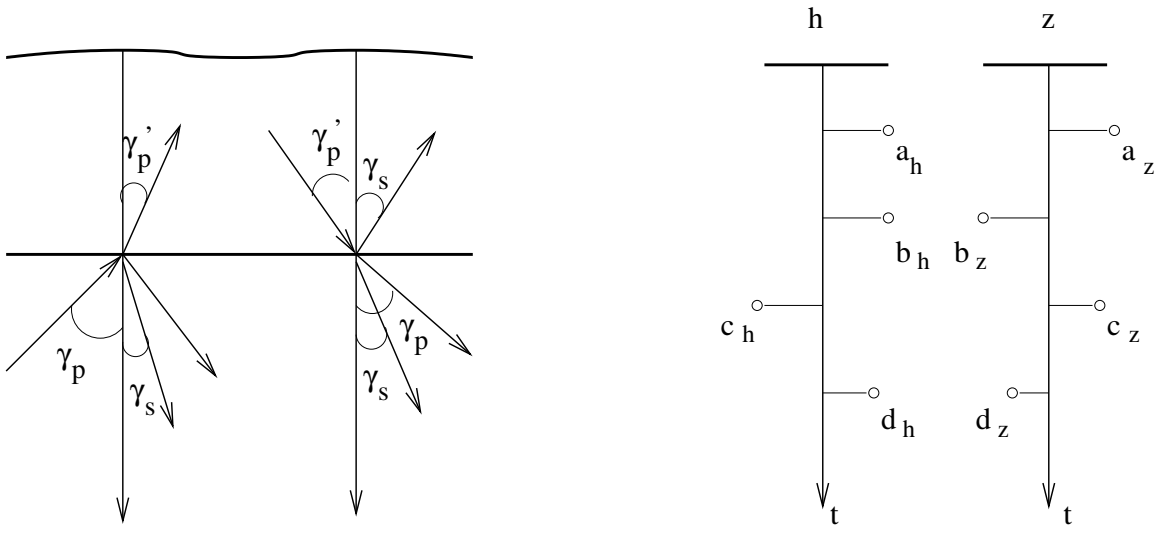

Figure 3: Physical model for the reverberations. It solves for the boundary conditions of the elastic wave field for the model on the left. On the right are shown the reverberations as a function of time for the hydrophone (h) and geophone (z) components. The first arrival corresponds to event a_h and a_z with an amplitude equal to a_h=kt, a_z=$\frac{kt}{\rho v_p}\cos\gamma_p'$. The first reverberation, b_h and b_z, has an amplitude of b_h=$-kt(1+kr)$ and b_z=$\frac{kt(1-kr)}{\rho v_p}\cos\gamma_p'$. The second reverberation, c_h and c_z, has an amplitude of c_h=$ktkr(1+kr)$ and c_z=$\frac{-ktkr(1-kr)}{\rho v_p}\cos\gamma_p'$. The third reverberation, d_h and d_z, has an amplitude of d_h=$-ktkr^2(1+kr)$ and d_z=$\frac{ktkr^2(1-kr)}{\rho v_p}\cos\gamma_p'$. daniel1-barrmod [NR]

calibrated geophone component ($\widehat{Z}=\frac{Z}{C}$,C is the calibration factor we need to compute):

$$\begin{aligned} P &= U+D, \\ Z &= \frac{U-D}{\rho v_p}. \end{aligned} \tag{2}$$

The initial source wavefield is given as follows:

$$S_0 = U_0 + D_0. \tag{3}$$

The propagated upgoing and downgoing wavefields at the water-bottom surface are, respectively,

$$\begin{aligned} U &= e^{\frac{-iw\Delta t}{2}}U_0, \\ D &= e^{\frac{iw\Delta t}{2}}D_0, \end{aligned} \tag{4}$$

where $\Delta t = 2\Delta z/v$, Δz is the water depth and v is the water velocity. From equations (3) and (4) the propagated source at the water-bottom surface is as follows:

$$S = D + e^{iw\Delta t}U. \tag{5}$$

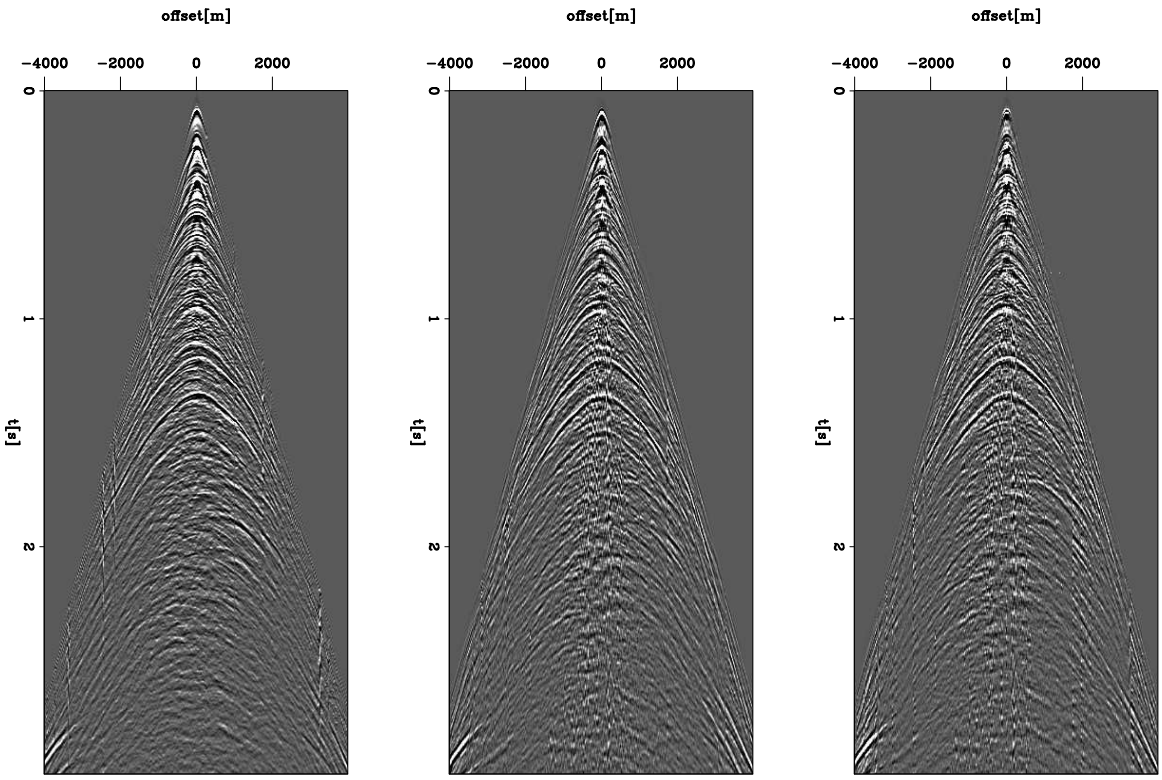

Figure 4: Hydrophone-geophone summation. From left to right: hydrophone component, geophone component, summation. daniel1-barr [CR,M]

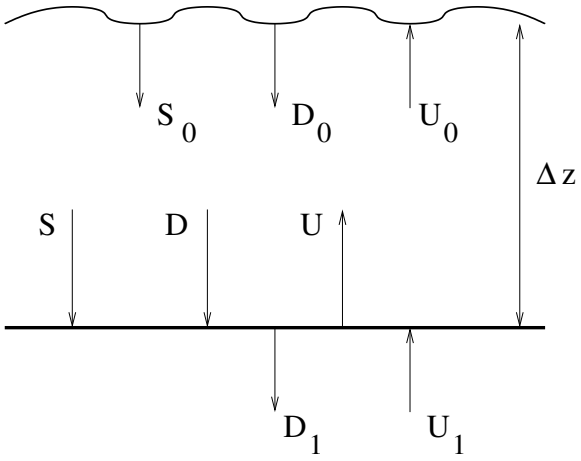

Figure 5: Physical model in study. From Soubaras (1996). daniel1-model [NR]

The calibration methodology assumes that the source energy should be zero after a time equal to the sum of the source-receiver propagation time and the source duration, which is a few hundred milliseconds. Combining equations (2) and (5) yields the following relation between the propagated source (S) and the hydrophone (P) and geophone (Z) components:

$$S = P' - CZ', \tag{6}$$

where:

$$\begin{aligned} P' &= \frac{1+e^{iw\Delta t}}{2}P, \\ Z' &= \frac{1-e^{iw\Delta t}}{2}Z. \end{aligned}$$

The propagated source vanishes after a certain period of time if the hydrophone and geophone are calibrated. This corresponds to finding C such that the propagated source (S) has minimum energy after a period of time:

$$\min_S \ ||S_{[a,b]}||^2. \tag{7}$$

The solution for this simple least-squares problem is as follows:

$$C = \frac{P'\overline{Z'}}{Z'\overline{Z'}+\epsilon^2}, \tag{8}$$

where ϵ is a small constant to avoid dividing by zero.

The filter C [equation (8)] is for a single trace. To obtain a filter for the entire gather, we compute the filter C for each trace and average them.

Figure 6 shows the hydrophone component of the receiver gather (left), the geophone component of the receiver gather (center) and the calibrated geophone (left).

Deghosting

After the calibration, the deghosting is as simple as taking the average between the hydrophone and calibrated geophone components:

$$U = \frac{P+Z}{2}. \tag{9}$$

Figure 7 compares the receiver gather of both the geophone component and the combined signal; observe that most of the ghost reflections have been eliminated. This can also be seen in the CMP gather of both the geophone component and the combined signal (Figure 8), where the arrows point to some of the multiples that have been removed.

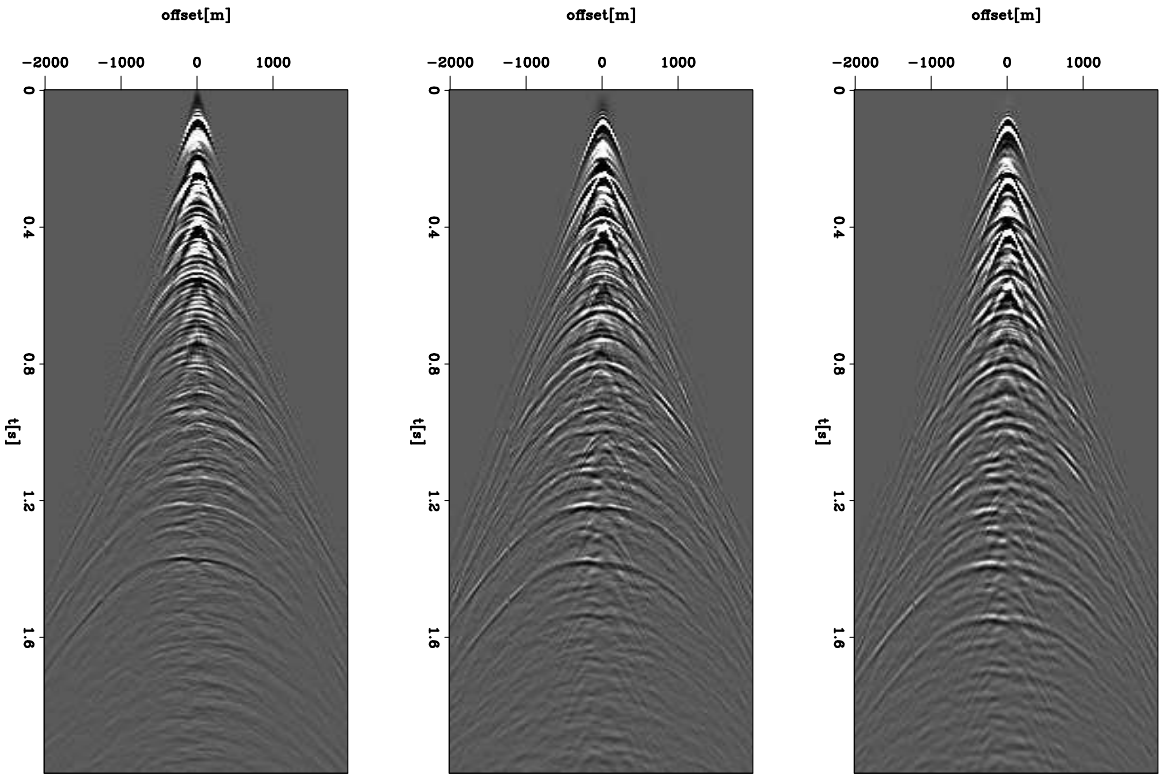

Figure 6: From left to right: hydrophone, geophone and calibrated geophone. daniel1-cal [CR,M]

MIGRATION RESULTS

The previous two sections show that the separate procedure of calibration and data combination provides better results than just calibrating and combining the data in one step. However, to verify whether we have effectively eliminated some multiples, we perform a poststack migration on the data and compare the results before and after the combination.

Wolf et al. (2004) propose a methodology that calculates stacking velocities without picking through a robust median estimator manufactured from neighboring traces only. The methodology depends on the estimation of the local step out; therefore, its accuracy strongly depends on the estimation of the dip field. Finally, the local estimate of the RMS velocity is:

$$V_{RMS}^2 = \frac{x}{t}\frac{dx}{dt} \tag{10}$$

The local step outs are estimated with Fomel (2000) method. Figure 9 shows the result of this methodology over three characteristic CMP gathers of the combined P-component Mahogany data set. From left to right, the figure shows the CMP gather, the dip field, and the RMS velocity function. The first CMP gather corresponds to the East part of the salt body, the second gather corresponds to the center part of the section, the third gather corresponds to the West part of the salt body. We estimate the velocity model for several CMPs, then perform linear interpolation and smoothing. Figure 10 shows the final slowness model.

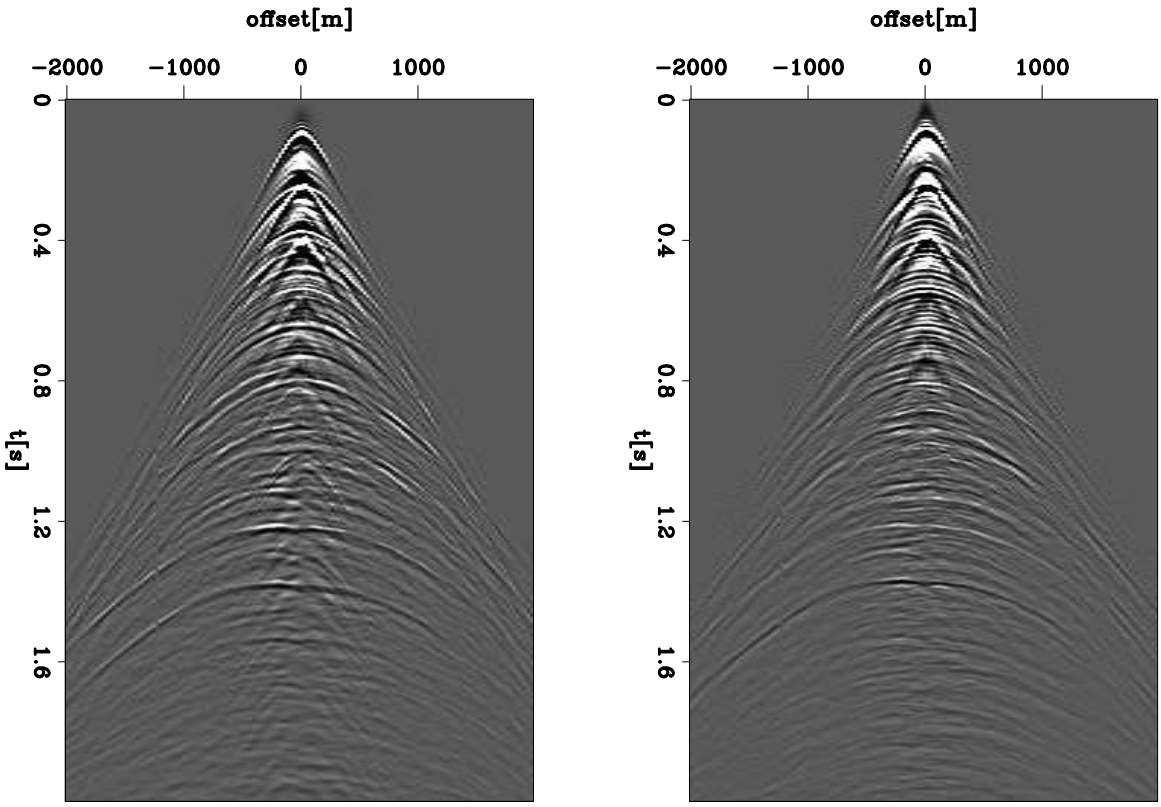

Figure 7: Geophone and deghosted gather, receiver gather. daniel1-deghost [CR,M]

Figure 11 presents the first 4000 m of the migrated seismic line. The top part shows the result of the combination and the bottom part shows the geophone component alone. In the same way, Figure 12 exhibits a close-up view of the migration result.

Several multiples have been attenuated; as indicated by the arrows in both Figures 11 and 12. This is an encouraging result; it reflects that our method produces a reasonable result. However, some multiples are still present in our final result. For example, notice the strong event that follows the water bottom reflection. Note that the water bottom can be considered flat, at a constant depth of approximately 118 m.

These multiples correspond to the source ghost. Further multiple-attenuation processes should be performed. For example, a wave-equation based multiple reduction technique can easily remove the source ghosts, since the water bottom is almost flat. This is a technique we have yet to test on this data set.

CONCLUSIONS

- Pseudo-unitary Radial-trace Transform can be used to successfully eliminate radial noise present in the hydrophone component of this 2D OBC line.

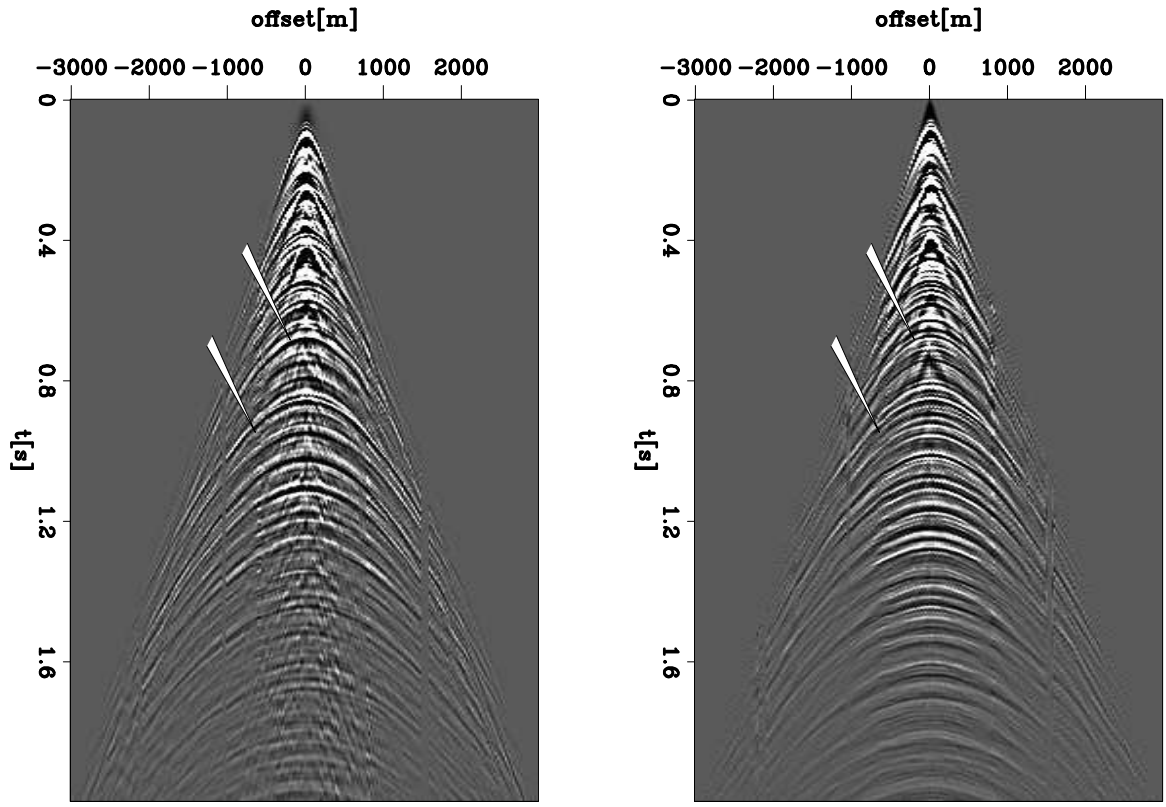

Figure 8: Geophone and deghosted gather, CMP gather. daniel1-cmps [CR]

- The time-domain methodology certainly removes some of the ghost energy. However, the frequency-wavenumber-domain method is more efficient in eliminating the ghost reflection, because it splits the geophone calibration and the receiver ghost elimination into two steps.

- We satisfactorily removed the receiver ghost on this data set, as is clearly shown in a comparison with the poststack migration result. However, further multiple-attenuation process is needed.

REFERENCES

Barr, F. J., and Sanders, J. L., 1989, Attenuation of Water-Column Reverberations Using Pressure and Velocity Detectors in a Water-Bottom Cable: 59th Ann. Internat. Meeting, Soc. Expl. Geophys., Expanded Abstracts, 653–656.

Brown, M., and Claerbout, J., 2000, Ground roll and the Radial Trace Transform - revisited: SEP–**103**, 219–237.

Fomel, S., 2000, Applications of plane-wave destructor filters: SEP–**105**, 1–26.

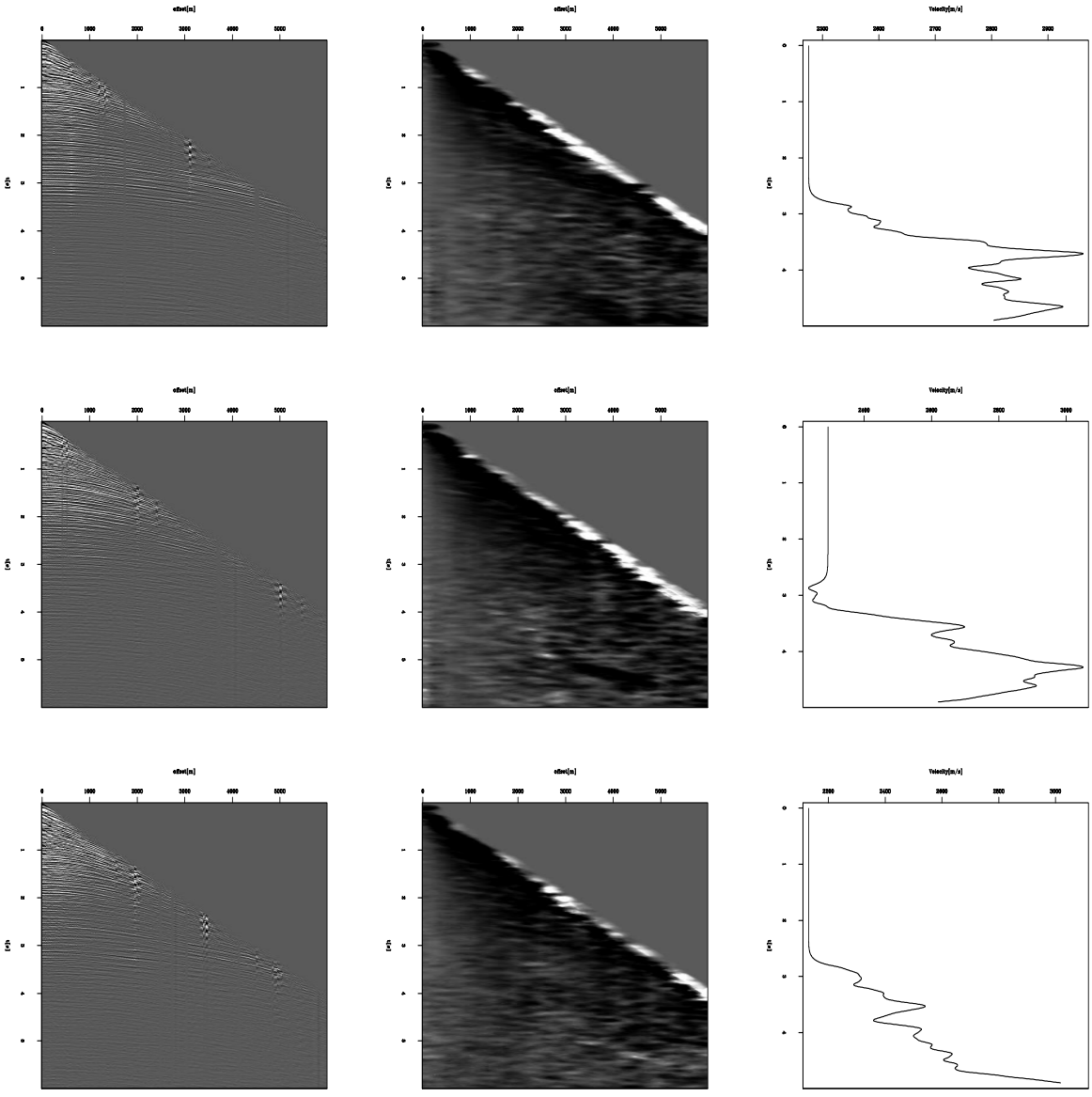

Figure 9: An example of the initial velocity model. From left to right: A typical combined CMP gather, dip field, RMS velocity function. From top to bottom, a gather taken from: The East part of the salt body, the center part of the section, the West part of the salt body. daniel1-vinit [CR]

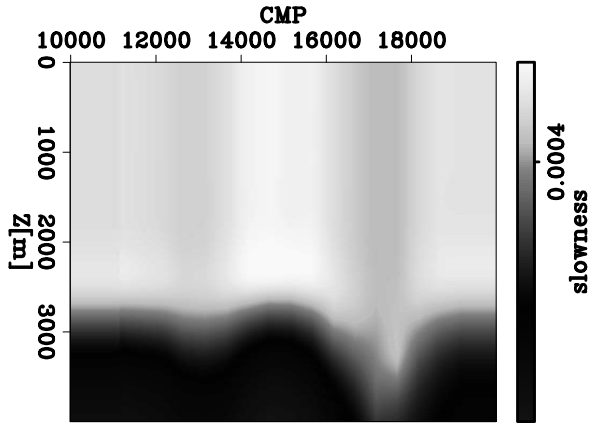

Figure 10: Initial P slowness model. daniel1-upslow [CR]

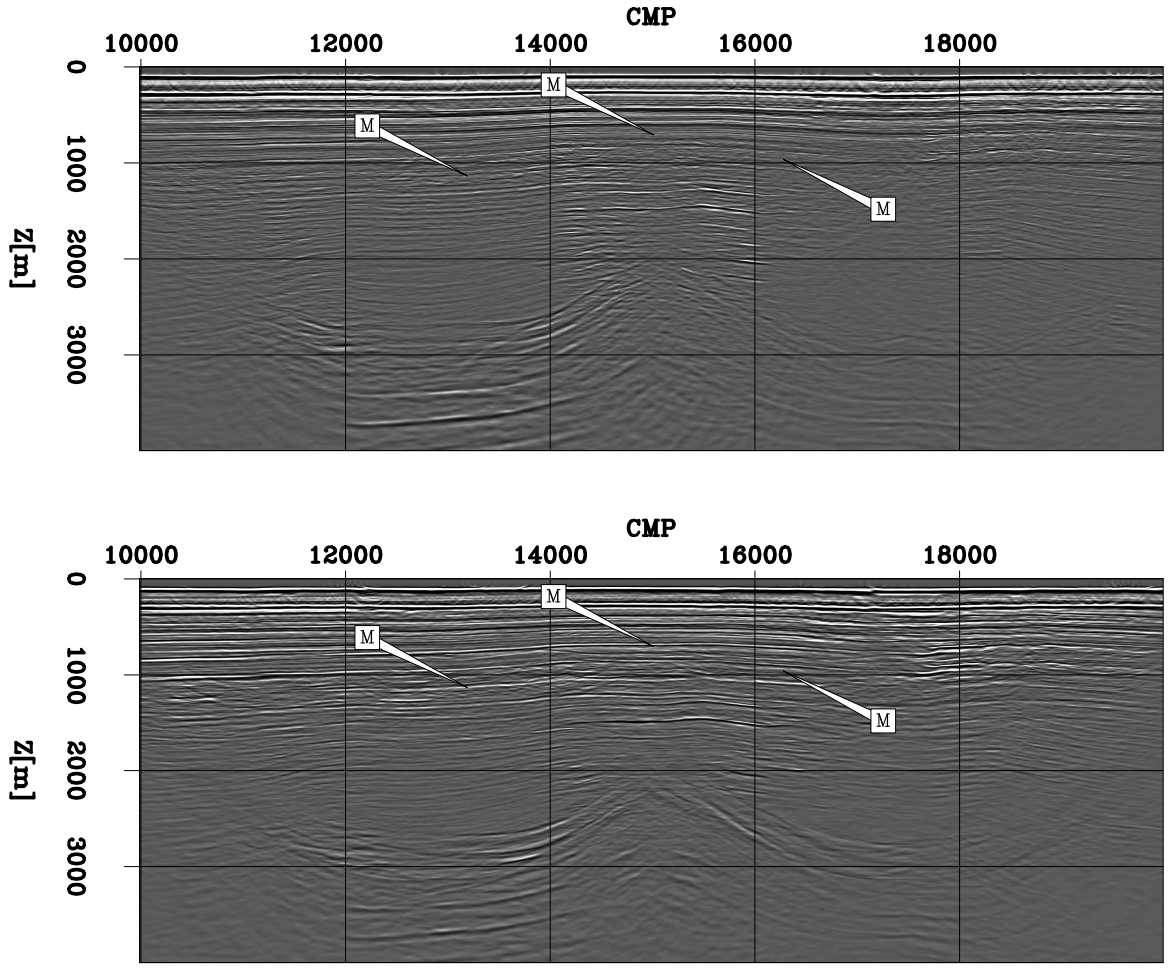

Figure 11: Comparison of the zero-offset section for the migration result of the combined signal (top) and the geophone component alone (bottom). daniel1-comp_mig [CR,M]

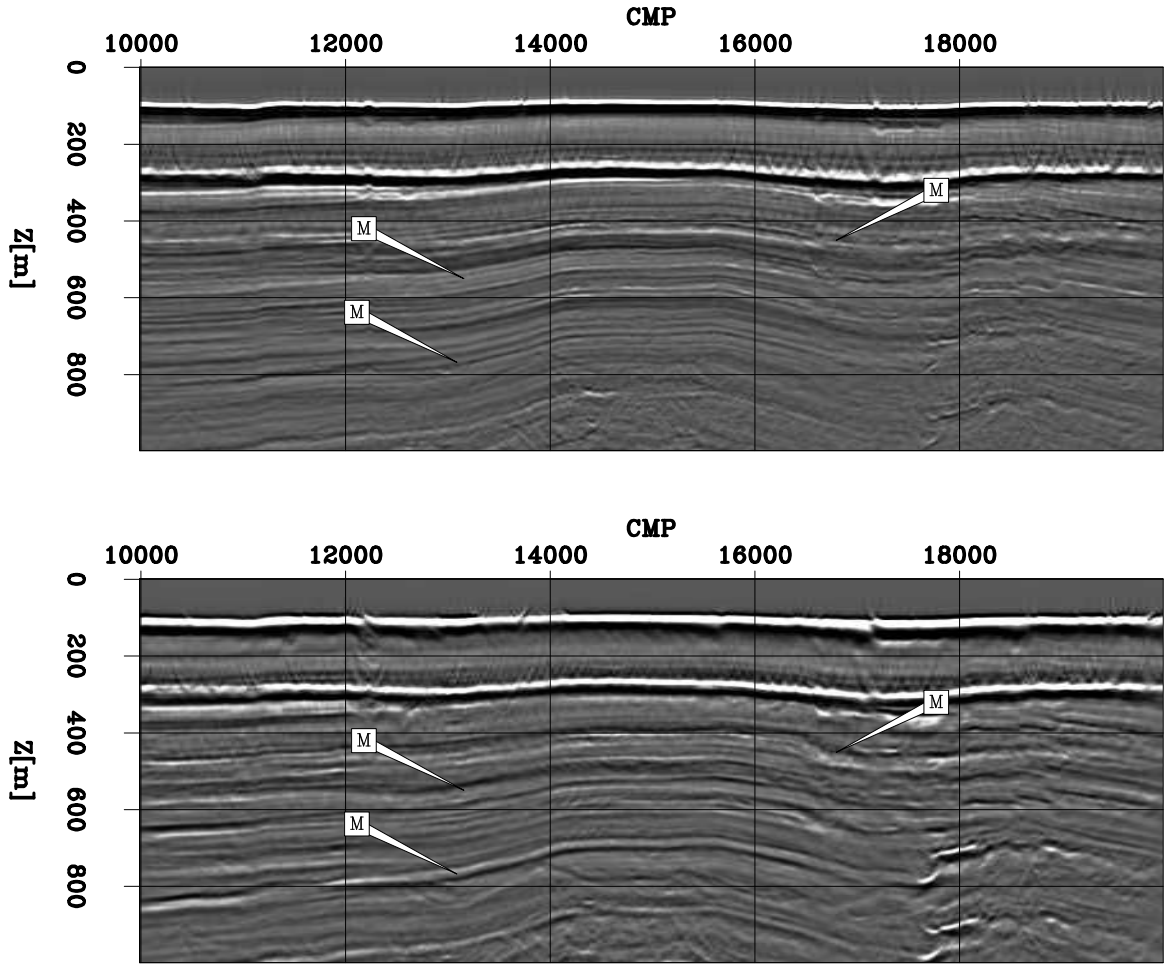

Figure 12: Detailed view of the migration result of Figure 11. daniel1-zoom_mig [CR,M]

Gal'perin, E. I., 1974 Soc. Expl. Geophys., Vertical Seismic Profiling: Society of Exploration Geophysicists Special Publication.

Soubaras, R., 1996, Ocean bottom hydrophone and geophone processing: 66th Ann. Internat. Meeting, Soc. Expl. Geophys., Expanded Abstracts, 24–27.

Wolf, K., Rosales, D., Guitton, A., and Claerbout, J., 2004, Robust moveout without velocity picking: SEP–**115**, 273–282.